World Journal of Clinical Cases

Submit a Manuscript: https://www.f6publishing.com

World J Clin Cases 2023 April 26; 11(12): 2637-2656

DOI: 10.12998/wjcc.v11.i12.2637

ISSN 2307-8960 (online)

MINIREVIEWS

Mediastinal lesions in children

Hasibe Gökçe Çinar, Ali Osman Gulmez, Çiğdem Üner, Sonay Aydin

Specialty type: Medicine, research and experimental

Provenance and peer review: Invited article; Externally peer reviewed.

Peer-review model: Single blind

Peer-review report's scientific quality classification

Grade A (Excellent): 0
Grade B (Very good): B; B
Grade C (Good): 0
Grade D (Fair): 0
Grade E (Poor): 0

P-Reviewer: Çolak E, Turkey

Received: December 15, 2022
Peer-review started: December 15, 2022
First decision: February 8, 2023
Revised: February 17, 2023
Accepted: March 24, 2023
Article in press: March 24, 2023
Published online: April 26, 2023

Hasibe Gökçe Çinar, Çiğdem Üner, Department of Pediatric Radiology, Ankara Etlik City Hospital, Ankara 06000, Turkey

Ali Osman Gulmez, Sonay Aydin, Department of Radiology, Erzincan Binali Yıldırım University Faculty of Medicine, Erzincan 24100, Turkey

Corresponding author: Ali Osman Gulmez, MD, Doctor, Department of Radiology, Erzincan Binali Yıldırım University Faculty of Medicine, Başbağlar, Hacı Ali Akın Cd. No. 32, Erzincan 24100, Turkey. aliosmangulmez.2@gmail.com

Abstract

The mediastinum is where thoracic lesions most frequently occur in young patients. The histological spectrum of diseases caused by the presence of several organs in the mediastinum is broad. Congenital lesions, infections, benign and malignant lesions, and vascular diseases are examples of lesions. Care should be taken to make the proper diagnosis at the time of diagnosis in order to initiate therapy promptly. Our task is currently made simpler by radiological imaging techniques.

Key Words: Mediastinum; Thoracic lesions; Vascular pathologies; Trachea and main bronchus pathologies; Esophageal pressure; Imaging in mediastinal lesions

Core Tip: The most common localization of thoracic lesions in children is the mediastinum. Pathologies arising from the presence of different organs in the mediastinum show a wide histopathological spectrum. Lesions may be congenital or include infections, benign and malignant lesions, and vascular pathologies. At the point of diagnosis, care should be taken at the point of starting the treatment quickly and making the correct diagnosis. Radiological imaging methods make our job easier at this point.

Citation: Çinar HG, Gulmez AO, Üner Ç, Aydin S. Mediastinal lesions in children. *World J Clin Cases* 2023; 11(12): 2637-2656
URL: https://www.wjgnet.com/2307-8960/full/v11/i12/2637.htm
DOI: https://dx.doi.org/10.12998/wjcc.v11.i12.2637

INTRODUCTION

The mediastinum is where thoracic lesions in children most frequently occur. A wide histological spectrum is present in pathologies caused by the presence of many organs in the mediastinum. Infections, benign and malignant lesions, and vascular diseases are examples of lesions, along with congenital lesions. Care should be made at the time of diagnosis to make the appropriate diagnosis and provide treatment as soon as possible. At this stage, our task is made simpler by radiological imaging techniques.

Individuals with mediastinal lesions may not have any symptoms, or they may have symptoms if the lesion has compressed or invaded into an organ nearby. Due to the most frequent injury to the trachea and main bronchi, anterior mediastinal lesions can result in edema of the upper extremities and face from superior vena cava compression and cyanosis in the neck veins, in addition to respiratory symptoms like cough, stridor, and dyspnea. Upper mediastinal lesions may result in Horner's syndrome, posterior mediastinal lesions may result in neurologic symptoms from spinal canal extension, and middle mediastinal lesions may cause dysphagia owing to esophageal compression.

IMAGING MEDIASTINAL LESIONS IN CHILDREN

The most common localization of thoracic lesions in children is the mediastinum. Pathologies arising from the presence of different organs in the mediastinum show a wide histopathological spectrum. Infections, benign and malignant lesions, vascular diseases, and congenital lesions are some examples of lesions[1]. Additionally, because the thymus is seen in young children in a variety of radiological manifestations, it can result in radiological findings that resemble masses.

Patients with mediastinal lesions may not experience any symptoms or may experience symptoms as a result of compression or invasion of the lesion into nearby organs. Because the trachea and major bronchi are most commonly damaged, anterior mediastinal lesions can cause respiratory symptoms such cough, stridor, and dyspnea, as well as edema of the upper extremities and face from superior vena cava compression and cyanosis in the neck veins. Middle mediastinal lesions may cause dysphagia due to esophageal compression, posterior mediastinal lesions may cause neurologic symptoms from spinal canal extension, and upper mediastinal lesions may cause Horner's syndrome[2,3].

Radiological imaging plays an important role in diagnosis, treatment planning and post-treatment follow-up. Direct photography is the first image technique to be employed. There are two ways to approach direct writing. Small lesions may not show up on radiographs, but larger lesions can show abnormal structures as well as an increase in density in the form of soft tissue mass, deterioration in mediastinal contours, and displacement in mediastinal lines[4,5]. The presence of ionizing radiation in direct radiography is its main drawback. However, for mediastinal lesions, its sensitivity in diagnosis is reported as 97%-100% and specificity as 36%[6,7].

The mediastinum is divided into compartments using categories to aid in the diagnosis and assessment of the localisation of various disorders. In the classification based on the lateral radiograph, the mediastinum is divided into three compartments as anterior, middle and posterior mediastinum (Figure 1). Accordingly, the anterior mediastinum is knowledgeable by the sternum anteriorly, the anterior edge of the pericardium posteriorly, the middle mediastinum by the pericardium anteriorly, the line passing 1 cm posterior to the anterior border of the thoracic vertebrae posteriorly, and the posterior mediastinum by the vertebral corpuscles behind this line and the posterior transverse processes[8].

Ultrasonography (US) is a preferred technique because it is simple to use and radiation-free. US is a recommended method since it is simple to use and radiation-free.

Multislice computed tomography (CT) is the most important imaging modality in the evaluation of mediastinal lesions. The most significant benefits include a shorter examination period, improved temporal and spatial resolution, enhanced anatomical clarity, and less respiratory artifacts. Additionally, as the examination time is cut down, so is the amount of time that kids are sedated. By obtaining thin-section images, high resolution multiplanar reformat, maximum intensity projection and volume rendering imaging techniques can be used to obtain images in three planes[9]. These advantages of CT, it plays an important role in evaluating the size, localization, density and contrasting pattern of the lesion, its characteristic features (fat, calcification fluid content) and its relationship with neighboring structures[4,10]. The most important disadvantage of the examination is radiation exposure.

The International Thymic Malignant Interest Group divided the mediastinum into prevascular (anterior), visceral (middle) and paravertebral (posterior) distances based on multislice CT (Figure 2). The paravertebral distance is the space between the vertebral bodies behind this line and the transverse processes posteriorly. The prevascular distance is defined as the space between the sternum anteriorly and the pericardium posteriorly. The visceral distance is defined as the line between the pericardium and 1 cm distal to the anterior border of the thoracic vertebrae. The thymus, adipose tissue, lymph nodes and left brachiocephalic vein are located in the prevascular distance, the heart, vascular structures, trachea, carina, esophagus and lymph nodes are located in the visceral distance, and the

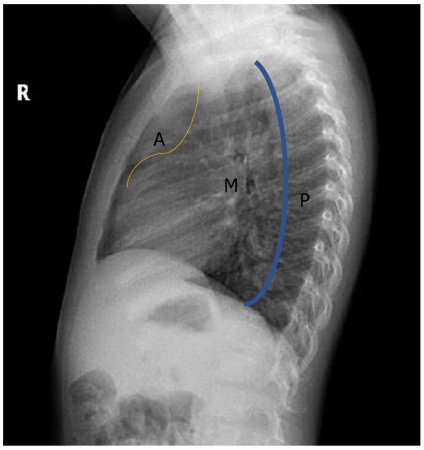

DOI: 10.12998/wjcc.v11.i12.2637

Figure 1 Mediastinal compartment classification on lateral radiograph. The borders of the mediastineal compartments anterior mediastinum are formed by the sternum anteriorly, the anterior edge of the pericardium posteriorly, the middle mediastinum by the pericardium anteriorly, the line passing 1 cm posterior to the anterior border of the thoracic vertebrae posteriorly, and the posterior mediastinum by the vertebral corpuscles behind this line and the posterior transverse processes. A (yellow line): Anterior; M: Middle; P (blue line): Posterior.

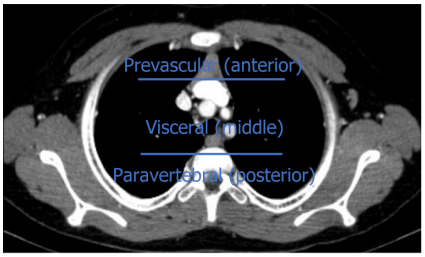

DOI: 10.12998/wjcc.v11.i12.2637

Figure 2 International Thymic Malignant Interest Group classification. In the axial computed tomography section passing through the superior aortic arch, the area between the sternum and the pericardium is the prevascular distance, the area between the pericardium and the line passing 1 cm distal to the anterior part of the vertebral corpus is the visceral distance, and the area posterior to this line is the paravertebral distance has been defined as.

thoracic vertebrae and paravertebral soft tissue are located in the paravertebral distance[10].

In magnetic resonance imaging (MRI), it gives more detailed information when compared to CT, especially when evaluated in terms of its high soft tissue contrast resolution and the absence of ionizing radiation in the examination. However, the long examination time, pulsation artifacts and the need for sedation in young children are the most important disadvantages. It also has low sensitivity in demonstrating calcifications[9,11,12]. MRI is a crucial imaging technique for mediastinal lesions, particularly for assessing the intraspinal extension of posterior mediastinal lesions, differentiating cystic-solid lesions, figuring out how lesions relate to the heart, pericardium, and great vessels, and demonstrating the cystic-necrotic components of solid lesions[13-15].

The differential diagnosis of mediastinal lesions is given in Tables 1, 2 and 3[16].

PREVASCULAR DISTANCE (ANTERİOR MEDIASTINAL) LESIONS

Thymus is the primary lymphoid organ and is responsible for T lymphocyte maturation. Since the thymus is prominent in infants and young children, it can lead to mass-like appearances on imaging. However, understanding the thymus' radiological characteristics and changes will be useful for making a differential diagnosis. Other anterior mediastinal abnormalities include thymic cyst, thymoma, thymic cancer, thymolipoma, and diseases invading the thymus.

The thymus is particularly prominent in children up to 3 years of age. Size decreases with age. It is located anterior to the superior mediastinum. In infants, it is observed in the form of square, homogeneous soft tissue density and bilobular appearance on direct radiographs. Its edges are convex or straight. Because of the neighborhood, the heart's outlines are removed. The hiluses cannot be chosen on the graph since they are superposed with them (Figure 3). The fact that it doesn't cause pressure is the most crucial characteristic[11,17]. It changes shape with breathing and position. It elongates and contracts in inspiration and shortens and expands in expiration. This finding is important in the differ-

Table 1 Prevascular space lesions

Prevascular space (anterior mediastinum)	Common	Less common
Thymus gland	Normal variations, thymic hyperplasia	Thymoma, thymic carcinomas
Lymphoma	Hodgkin and non-hodgkin lymphoma	
Germ cell tumor	Mature teratoma	Immature teratoma, seminoma, nonseminoma tumors
Thyroid		Intrathoracic goiter
Lymph node enlargement	Benign etiology	Malignant etiology
Cystic masses	Thymic cyst, lymphatic malformation	
Fatty lesions		Thymolipoma and lipoma

Table 2 Visceral space lesions

Visceral space (middle mediastinum)	Common	Less common
Vascular lesions	Vascular ring, pulmonary sling, aneurysm	Pseudoaneurysm
Lymph node enlargement	Benign: Infection	Malignant: Primary or secondary
Foregut duplication cyst	Bronchogenic cyst, esophageal duplication cyst, neuroenteric cyst	

Table 3 Paravertebral space lesions

Paravertebral space (posterior mediastinum)	Common	Less common
Sympathetic ganglia tumor	Neuroblastoma, ganglioneuroma, ganglioneuroblastoma	
Peripheral nerve sheath tumor		Schwannoma, neurofibroma, malignant peripheral nerve sheath tumor
Non neurogenic tumors	Lymph node enlargement, vascular malformation or aneurysm	Extramedullary hematopoiesis, small round blue cell malignancies

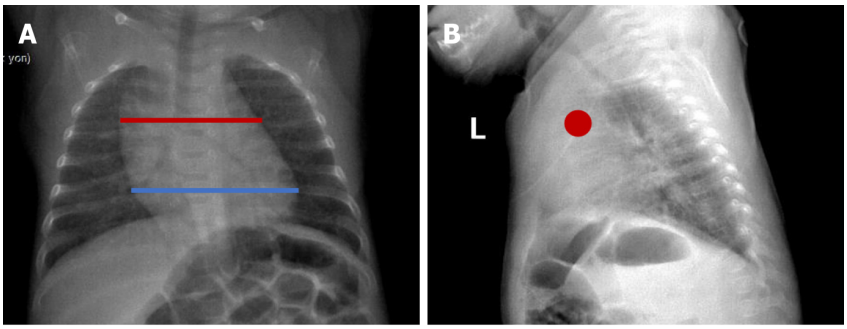

DOI: 10.12998/wjcc.v11.i12.2637

Figure 3 A 3-year-old boy normal thymus. A: The red line shows the thymus and the blue line shows the heart in the posteroanterior chest radiograph. In infants, the thymus erases the heart contours, and because it is superposed with the hiluses, the hiluses cannot be clearly distinguished. It also does not create a compression effect. B: Anterior location of the thymus is observed with a red dot on the lateral radiograph.

ential diagnosis of solid masses and infiltrative processes, especially in real-time examinations such as US[18].

The thymus can be seen in many different forms on direct radiographs and other radiological images. The wave sign is the appearance of a corrugation on the edge of the thymus at the point where it rests on the ribs (Figure 4). When the right lobe of the thymus is triangular and the minor fissure forms its lower boundary, the sail sign is the result (Figure 5). The cardiothymic notch is the notch that occurs at the junction of the heart and thymus (Figure 6).

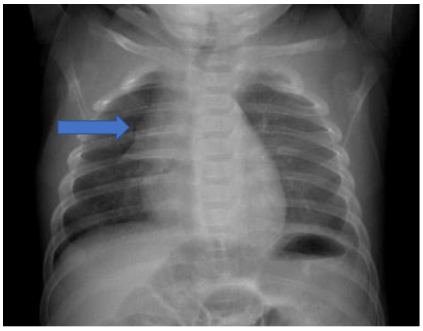

DOI: 10.12998/wjcc.v11.i12.2637

Figure 4 The wave sign (blue arrow) is the corrugation view of the right lobe of the thymus due to its abutment to the ribs.

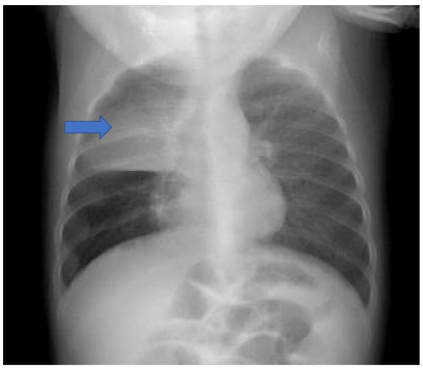

DOI: 10.12998/wjcc.v11.i12.2637

Figure 5 Sail sign (blue arrow) is the triangular shape of the right lobe of the thymus and the minor fissure forming its lower border.

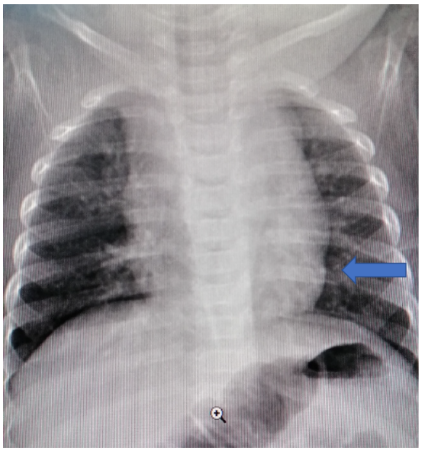

DOI: 10.12998/wjcc.v11.i12.2637

Figure 6 The contour (blue arrow) formed at the junction of the thymus with the heart is the cardiothymic notch.

In CT, the thymus is observed in the anterior-upper mediastinum, anterior to the main vascular structures and pericardium. In infants and young children, it is in the form of a solid structure with convex edges and homogeneous density, which does not create a compression effect. As the age increases, the edges become flat or concave, while in adolescence, it is observed as a triangular shape with a reduced size[19] (Figures 7-9). In a study on this subject, it was discovered that the thymus, which has a median location and straight lateral contours, is the most prevalent morphological shape in children. The thymus's average transverse and anterior-posterior dimensions were 30 ± 11 mm and 17 ± 5 mm, respectively. The average thymic lobes' width and thickness were roughly 21 ± 5 and 15 ± 7 mm for the right and 26 ± 8 and 15 ± 6 mm for the left, respectively. The anterior-posterior diameter of the thymus was not substantially correlated with age, however the transverse diameter and thymic lobe dimensions of the thymus decreased dramatically with age. Despite the fact that girls' mean thymic attenuation values were higher than boys', this gender difference was not statistically significant[20].

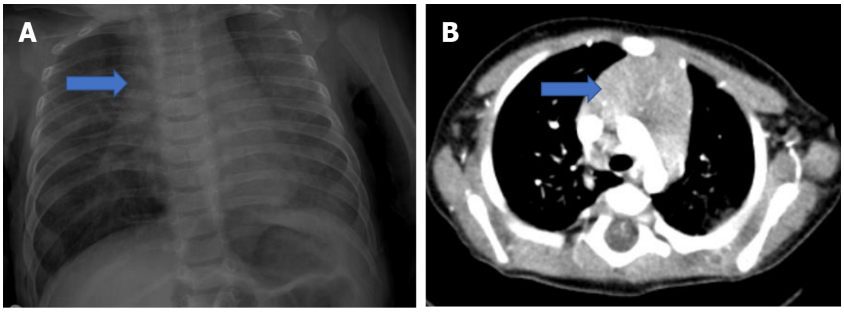

DOI: 10.12998/wjcc.v11.i12.2637

Figure 7 Normal thymus and axial computed tomography of a 4-mo-old patient. A: Normal thymus on posteroanterior chest radiograph; B: Axial computed tomography (CT) examination of a 4-mo-old patient. In CT, the thymus (blue arrow) arcus is observed in the prevascular distance at the level of the aorta, its edges are convex, with homogeneous density and it does not cause a compression effect.

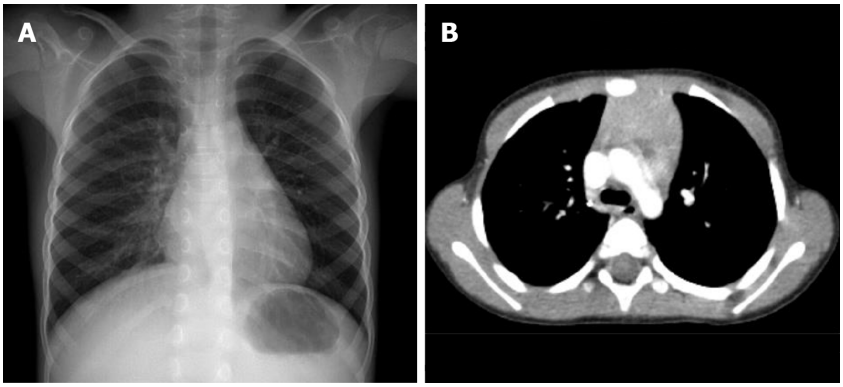

DOI: 10.12998/wjcc.v11.i12.2637

Figure 8 A 4-year-old patient's posteroanterior chest radiograph. A: It shows a decrease in the dimensions of the thymus; B: Flattened edges in the axial computed tomography examination.

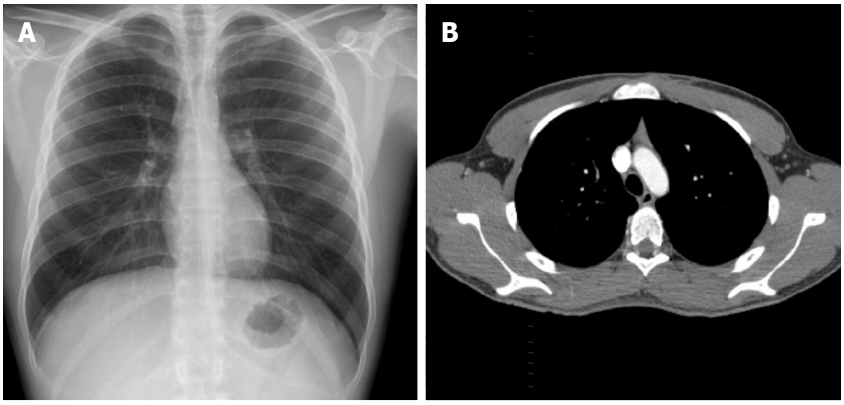

DOI: 10.12998/wjcc.v11.i12.2637

Figure 9 A 17-year-old patient's examination. A: Thymus is not observed in the posteroanterior chest radiograph of the 17-year-old patient; B: In the axial section, on computed tomography, it is observed as small, triangular in the anterior mediastinum, with concave edges and lower density due to the fat tissue it contains.

One of the rare variations of the thymus that creates a mass appearance on the radiograph is the extension of the thymus to the superior vena cava and posterior to the great arteries[21] (Figure 10).

Thymic hyperplasia, one of the pathologies of the thymus, is seen in two forms as true and lymphoid hyperplasia. The development of atrophy in the thymus as a result of stresses such as systemic infection, burns, chemotherapy, and an increase in thymus size within a period of a few months to two years when the stress is removed is true hyperplasia. It may develop in lymphoid hyperplasia without expanding in size, and a rise in the number of lymphoid follicles is found[22]. It may be associated with autoimmune diseases. In cross-sectional examination, an increase in size is detected in the thymus.

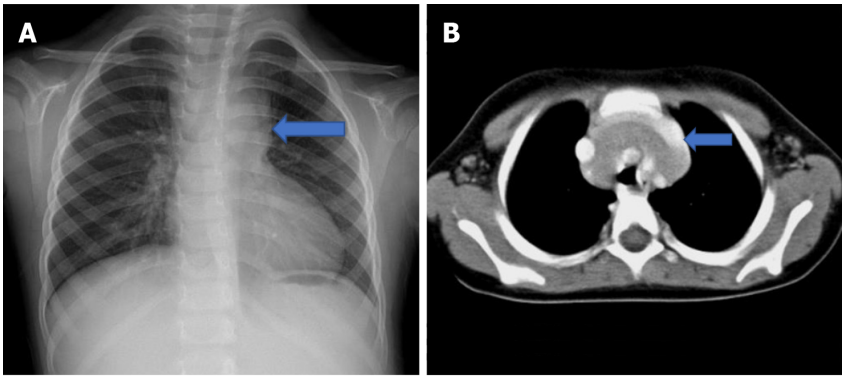

DOI: 10.12998/wjcc.v11.i12.2637

Figure 10 A 3-year-old patient who presented with the complaint of cough. A: There is mediastinal enlargement on the left in the posteroanterior chest radiograph; B: In the axial computed tomography examination, it is observed that the thymus forms the mediastinal enlargement and the thymus (blue arrow) extends to the posterior of the main vascular structures.

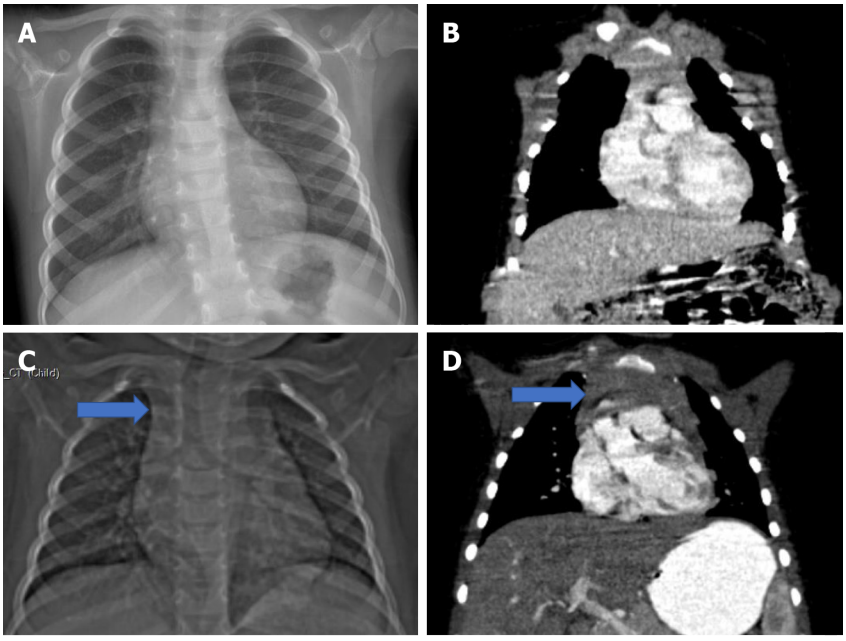

DOI: 10.12998/wjcc.v11.i12.2637

Figure 11 A 3-year-old patient who was followed up with an operated Wilms tumor during chemotherapy. A: The thymus tissue is observed to be smaller than normal in the posteroanterior chest radiograph; B: Coronal computed tomography examination; C and D: In the second month follow-up of the same patient after the end of chemotherapy. Hyperplasia in the thymus (blue arrow) is observed in the scout (C) and coronal plane computed tomography images (D).

Lobulation can be observed in the contour. However, its density is homogeneous. It does not contain necrosis or calcification (Figure 11). Since the thymus contains adipose tissue histopathologically, measuring the chemical shift ratio in in-phase-out-phase sequences in MRI examination has an important place in distinguishing the thymus from the mass. A chemical shift ratio of less than 0.9 indicates normal thymus tissue[23].

THYMIC PATHOLOGIES

Thymic cyst is one of the rare benign pathologies of the thymus. Radiologically, they are observed with smooth contours, fluid density and homogeneous content. They do not contain solid components. However, an increase in their density may be detected due to hemorrhage or proteinaceous content. It can be unilocular or multilocular. Congenital cysts develop in the anterior mediastinum or neck along the thymopharyngeal canal[22]. It is usually unilocular. Acquired cysts can be seen in patients with Hodgkin lymphoma and autoimmune diseases, trauma, thoracotomy and radiotherapy-chemotherapy [22,23] (Figure 12). Those originating from thymoma or thymic carcinoma from the cyst wall have also been reported in the literature[24,25] (Figure 12). Thymoma is an epithelial tumor and is seen in less

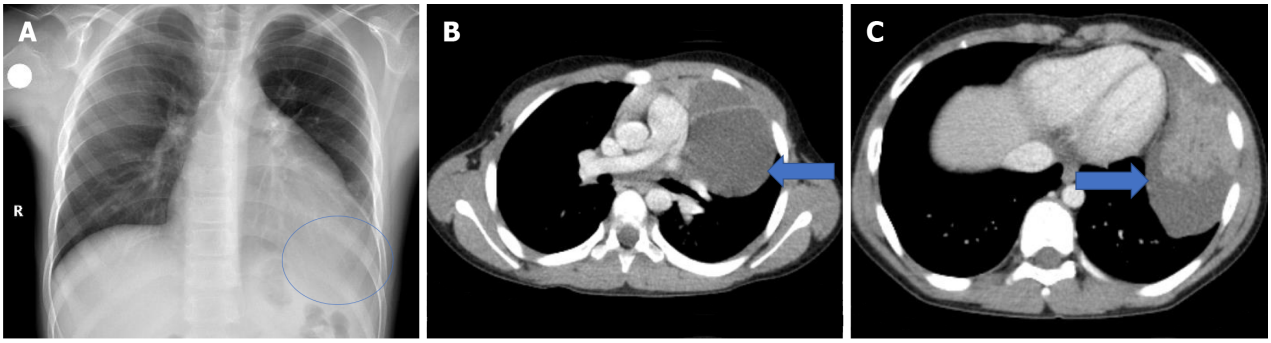

DOI: 10.12998/wjcc.v11.i12.2637

Figure 12 A 10-year-old patient who is being followed up for asthma. A: Density that erases the heart and diaphragm contours (blue round) on the left is observed on posteroanterior chest radiography; B: Thymic cyst containing septa (blue arrow); C: A solid component of the thymoma (blue arrow) in the inferior of the cyst are observed.

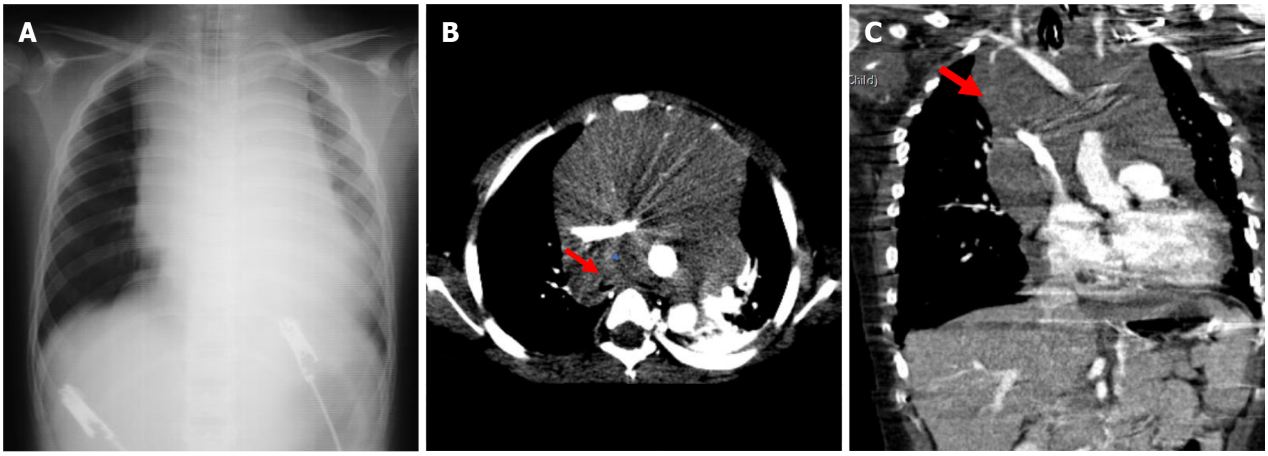

DOI: 10.12998/wjcc.v11.i12.2637

Figure 13 A 5-year-old patient with T-cell ALL has neck and back pain, shortness of breath, and cough. A: On posteroanterior chest radiograph, significant enlargement of the mediastinum secondary to the mass and increased aeration in the right lung are observed; B: Compression of the right main bronchus secondary to the mass (red arrow) also draws attention; B and C: A mass lesion (red arrow) located in the anterior mediastinum but extending into the middle mediastinum and circulating the main vascular structures is observed.

than 1% of children[26]. It is associated with myasthenia gravis at a rate of 5%-15%[27]. There are two types, non-invasive and invasive. While it is observed as a smooth, homogeneous, solid lesion on CT, irregular contours, calcification and necrosis, heterogeneous enhancement, and pleural invasion should suggest the invasive type[16,19].

Thymic carcinoma is rare in children[18]. Similar radiological findings to invasive thymoma are obtained by CT. It's a tumor that grows quickly.

When illnesses affect the thymus, it manifests as a mediastinal mass. Acute leukemia is the first one of these illnesses. The most common cancer in children is leukemia and constitutes 30% of childhood cancers[27,28]. Acute lymphoblastic leukemia (ALL) constitutes 85% of acute leukemias and can be seen at any age, but is most common between 2-5 years of age. Eighty-five percent of ALL is of B cell origin and 15% is T cell origin[29]. Mediastinal mass due to leukemic infiltration of the thymus, compressive results due to the mass, and pleural effusion are frequently seen in T-cell lymphoblastic leukemia[30] (Figure 13). The same radiological findings occur in T-cell lymphoblastic lymphoma (Figure 14). The differential diagnosis between the two pathologies is made according to bone marrow involvement. In T-cell lymphoblastic lymphoma, less than 20% of blasts are detected in the bone marrow. Both T-cell ALL and T-cell lymphoblastic lymphoma are aggressive and rapidly progressive pathologies. Therefore, the diagnostic phase should be rapid[31].

Another pathology that infiltrates the thymus is Langerhans cell histocytosis. It is frequently seen with multisystemic disease in children under the age of one. It occurs as thymus infiltration and/or mediastinal lymph node involvement and its incidence is reported to be 2.6%[32]. Isolated cases have also been published in the literature. CT findings of thymic infiltration are heterogeneous appearance secondary to enlargement, nodular contour, calcification and cystic changes in the thymus (Figures 15 and 16A and B). The presence of punctate calcifications and the appearance of air cysts should suggest langerhans cell histiocytosis. Differential diagnosis with teratoma should also be made because it

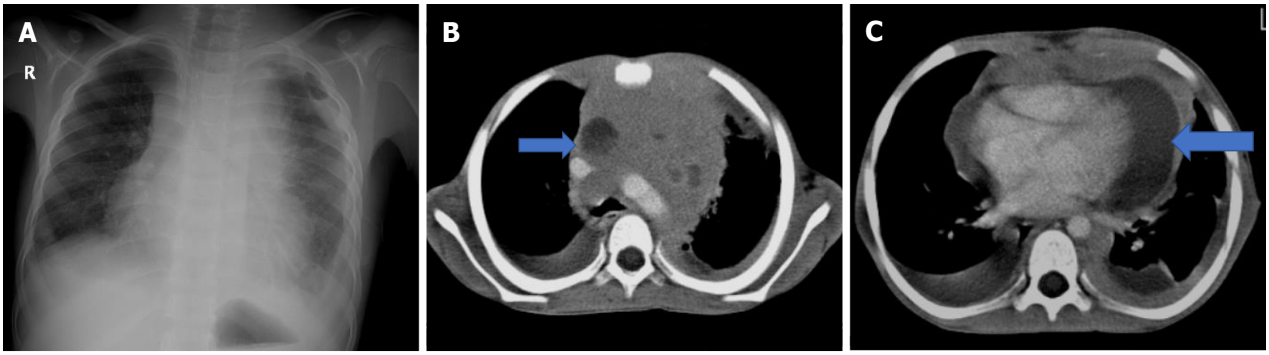

DOI: 10.12998/wjcc.v11.i12.2637

Figure 14 A 7 years old patient with T-cell lymphoblastic lymphoma. A: There is cough and shortness of breath. Significant enlargement of the mediastinum, pleural effusion in the left hemithorax, and increased aeration in the right lung are observed in the posteroanterior chest radiograph; B and C: In the axial computed tomography examination, a mass lesion with fatty areas is located in the anterior mediastinum. Bilateral pleural and pericardial effusion, and pleural and pericardial fatty solid lesions (blue arrow) are also observed.

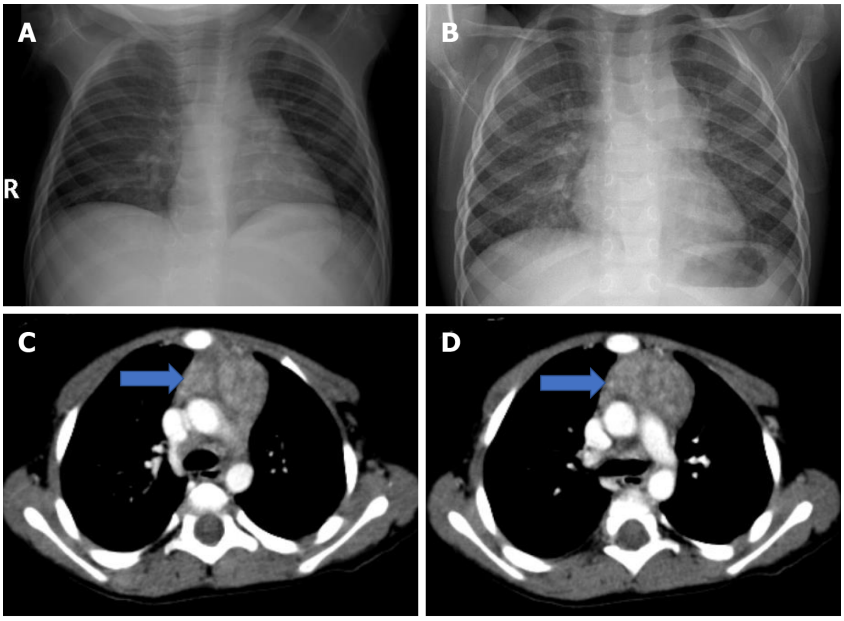

DOI: 10.12998/wjcc.v11.i12.2637

Figure 15 In the 1 year and 9 mo old patient with langerhans cell histiocytosis. A: The first one; B: The second radiograph taken six months after A, Mediastinal enlargement and lobulation in the left mediastinal contour are observed; C and D: Thymic enlargement (blue arrow), lobulation in the contour and heterogeneous appearance are observed in the axial computed tomography images of the same patient.

contains calcifications[19,33,34].

LYMPHOMA

Lymphoma is the most common tumor of the anterior mediastinum in children. Although non-Hodgkin lymphoma is more common in children, the incidence of anterior mediastinal mass is more common in Hodgkin lymphoma[35]. Mediastinal involvement is seen either as a mass secondary to thymic infiltration or as lymphadenopathies due to lymph node involvement (Figures 16C and D, 17, and 18A and B). In thymic infiltration, mediastinal enlargement and compression findings are detected on chest radiograph. Contrarily, CT might be viewed as a pressure-forming mass with lobulated outlines and necrotic patches. Although calcification is rare, calcification may develop after treatment[16,36]. Pulmonary nodules and pleural effusion may accompany the findings at a rate of 5% in Hodgkin lymphoma[35].

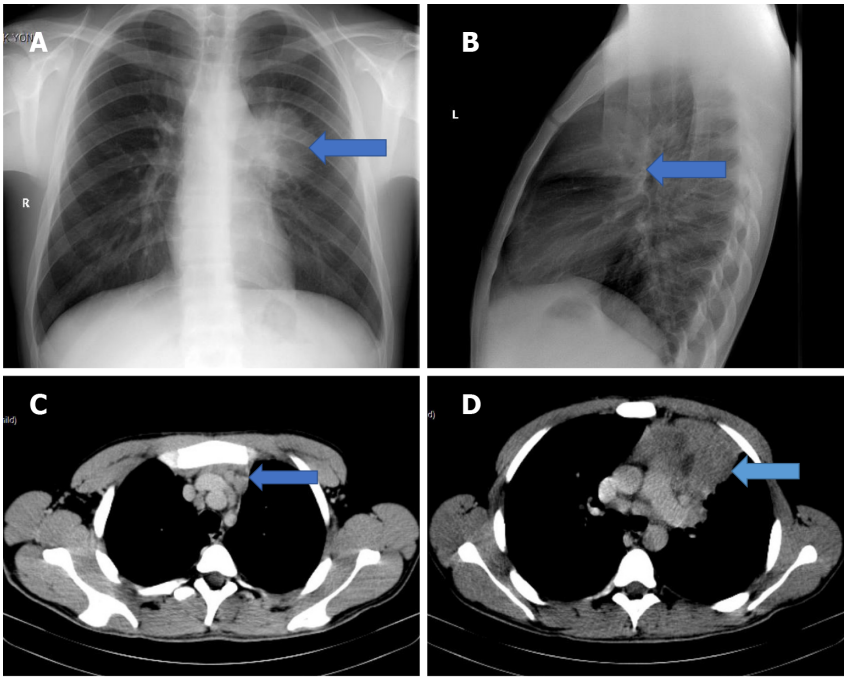

DOI: 10.12998/wjcc.v11.i12.2637

Figure 16 Hodgkin lymphoma (nodular sclerosing type). A 17-year-old male patient presents with cough and weight loss. A and B: On the 2-way chest radiograph there is a mass density (blue arrow) located in the anterior mediastinum; C: Lymphadenopathies (blue arrow) in the upper mediastinum; D: A mass lesion containing cystic-necrotic areas (blue arrow) in the anterior mediastinum are detected.

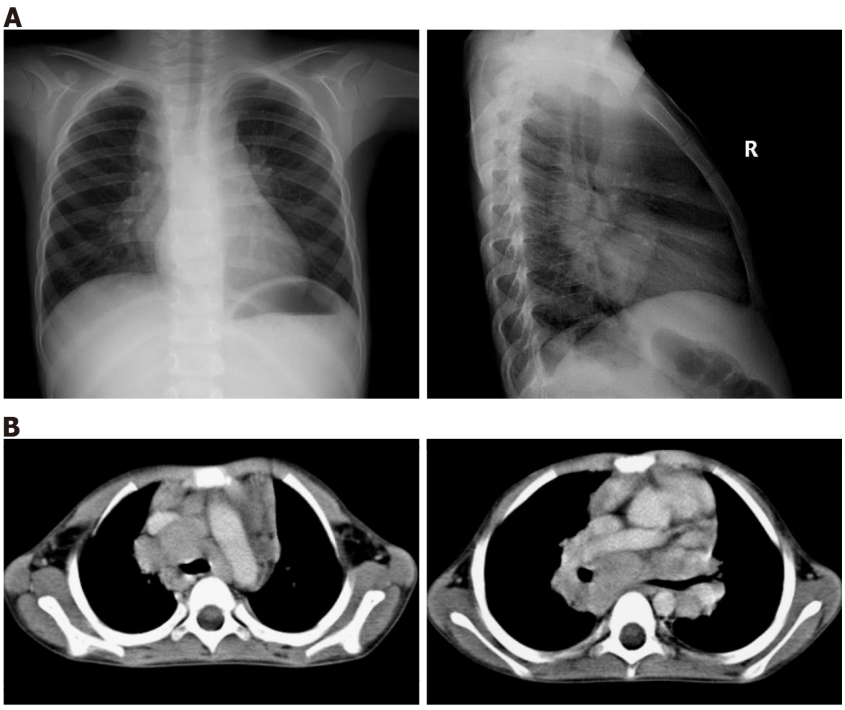

DOI: 10.12998/wjcc.v11.i12.2637

Figure 17 4-year-old male patient with Hodgkin lymphoma (mixed cellular type). A: Mediastinal enlargement and bilateral hilar lymphadenopathy are observed in the 2-way chest radiograph of the patient with the complaints of fever and anemia; B: Lymphadenopathies forming conglomeration in prevascular, paratracheal, subcarinal, hilar and azygoesophageal recess are observed in the axial computed tomography images of the same patient.

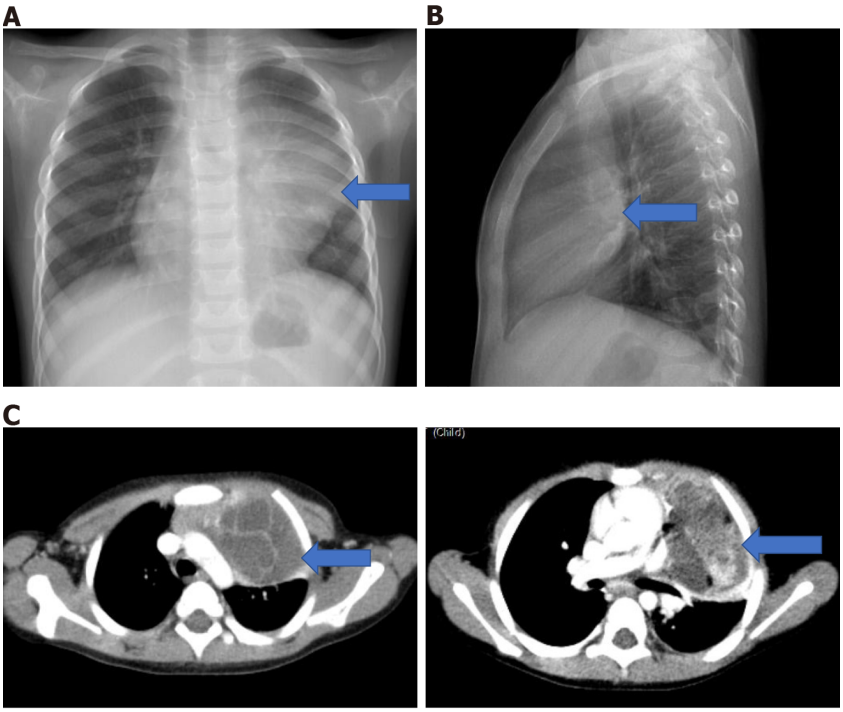

DOI: 10.12998/wjcc.v11.i12.2637

Figure 18 A 3-year-old girl with mature teratoma. She presents with dyspnea. A: On the posteroanterior chest radiograph the mass (blue arrow) erases the contour of the hilus and heart on the left, slightly compresses the left main bronchus; B: It is located in the anterior mediastinum on the lateral X-ray (blue arrow); C: In the axial computed tomography images of the same patient, a septated mass lesion containing fluid, calcification and fat density (blue arrow) is located in the anterior mediastinum, it compresses the thymus and slightly compresses the left main bronchus. The mass also extends to the left side of the mediastinum.

GERM CELL TUMORS

The most common location of extragonadal germ cell tumors is anterior mediastinum and constitutes 6%-18% of all mediastinal masses[37]. It is located in the thymus or adjacent to the thymus. However, they can also originate from the heart and pericardium, and they may rarely be located in the posterior mediastinum[38]. They peak in the two-year-old period, the first 2 years and the adolescence period [39]. Eighty percent of these tumors are benign and the most common type is teratoma. Teratomas are divided into two groups as mature and immature. Teratomas are observed radiologically as smooth, round or lobulated contours. Fat, calcification and fluid densities are observed in cross-sectional examination. Calcification is observed in 1 or 2 cases out of 5.

These tumors extend to one side of the midline[40] (Figure 18). The lesion should be flagged as an immature teratoma if it is big and diverse, invades nearby tissues, comprises soft tissue components, and is necrotic and hemorrhagic[16,21]. Seminoma and non-seminomatous germ cell tumors (yolk sac tumor, embryonal carcinoma, choriocarcinoma, and mixed type) are less common. They are observed as large masses on direct graphy. However, in cross-sectional examination, seminomas are observed as solid masses of homogeneous density, and they can also metastasize to regional lymph nodes and bone [16]. Although non-seminomatous lesions are observed more heterogeneously due to necrosis and hemorrhage, they may also invade neighboring structures[41]. In addition, non-seminomatous tumors have a more aggressive course and metastases are detected in 85%-95% of them at the time of diagnosis [42]. High levels of B-HCG and AFP are also important laboratory findings in the diagnosis of non-seminomatous tumors. Germ cell tumors may also be associated with Kleinefelter syndrome[43] (Figure 19).

INTRATHORACIC GOITER

It is rarely seen in children. It is located in the anterior mediastinum with a rate of 75%-90% and in the posterior mediastinum with a rate of 10%-25%[44]. It is observed as tracheal deviation or compressive density on direct graphy (Figures 19C and D, and 20). In order to show tracheal compression, cross-sectional examinations are better to direct radiography. They are crucial for preoperative evaluation[14].

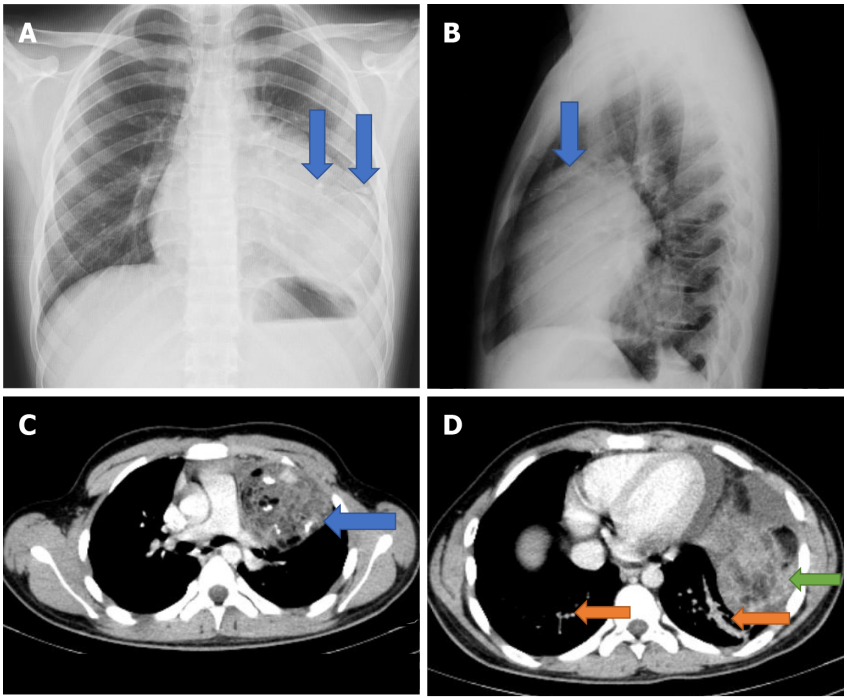

DOI: 10.12998/wjcc.v11.i12.2637

Figure 19 A 14-year-old male patient with Kleinefelter syndrome. He has been complaining of pain in the left arm and shoulder for 3 d. A: Posteroanterior chest radiograph shows calcifications (double blue arrow) that erases the contour of the heart; B: Diaphragm on the left and the density of a mass located in the anterior mediastinum on the lateral radiograph (blue arrow); C: In the axial computed tomography images of the same patient, a lobulated mass lesion with calcification, fluid and fat densities, located in the left anterior mediastinum, adjacent to the thymus is observed (blue arrow); D: Pericardial and pleural effusion are present in the inferior slices of the same patient (green arrow). In addition, basal linear atelectasia is (double orange arrow).

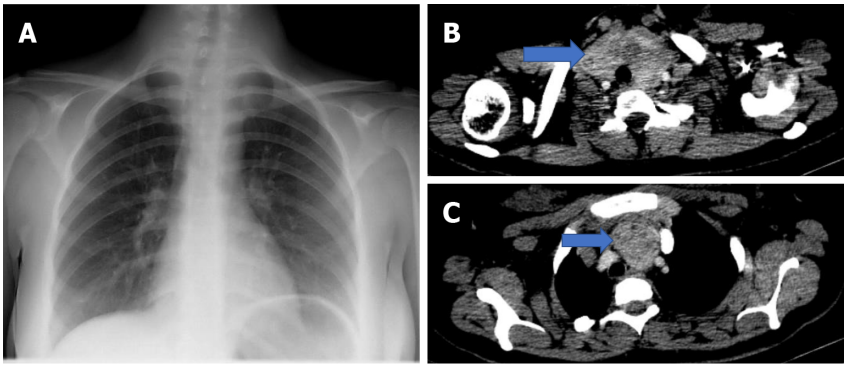

DOI: 10.12998/wjcc.v11.i12.2637

Figure 20 A 17-year-old girl with intrathoracic goiter. A: In the posteroanterior chest radiograph of the patient followed up for multinodular goiter, enlargement in the upper mediastinum and a density that deviates the trachea to the right are observed. B and C: In axial computed tomography images (blue arrow), the thyroid gland is hyperplastic and contains nodules. In addition its extension is observed in the anterior mediastinum up to the superior aortic arch. Trachea is deviated to the right and no compression is detected.

VISCERAL DISTANCE (MIDDLE MEDIASTINAL) LESIONS

Visceral space lesions are divided into vascular and non-vascular lesions. Childhood vascular lesions lead to congenital abnormalities. Double aortic arch, left aberrant subclavian artery associated with the right aortic arch, right aberrant subclavian artery associated with the left aortic arch, pulmonary artery sling, and double superior vena cava are among these anomalies[16,21] (Figure 21). Thoracic aortic aneurysms are seen in hereditary diseases (Marfan syndrome, Loeys-Dietz syndrome, Aortic tortiosity syndrome, Ehler Danlos syndrome, Cutis laksa syndrome, Noonan syndrome and Alagille syndrome) and congenital heart diseases (aortic coarctation, bicuspid aorta, Fallot tetralogy)[45] (Figures 22 and 23).

Vascular lesions are seen as a mediastinal mass at a rate of 10% on direct X-ray and may present as mediastinal enlargement, increased density, tracheal compression, or thickening of the mediastinal lines. The most effective method in diagnosis is CT Angiography[46].

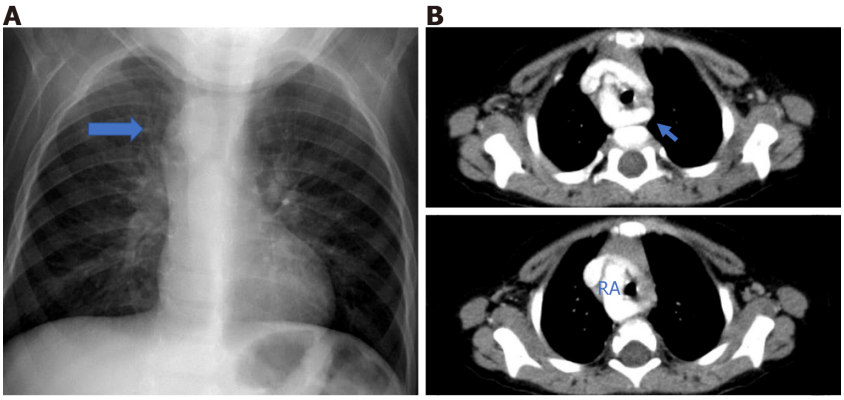

DOI: 10.12998/wjcc.v11.i12.2637

Figure 21 A 2-year-old male patient with right aortic arch. A: There are complaints of shortness of breath and cough. On posteroanterior chest radiograph, enlargement of the upper mediastinum on the right and compression of the trachea are observed (blue arrow); B: Right aortic arch and left aberrant subclavian artery (blue arrow) are observed in the axial computed tomography angiography images of the same patient. RA: Right aortic arch.

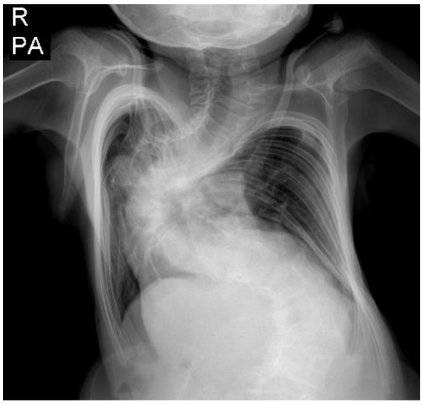

DOI: 10.12998/wjcc.v11.i12.2637

Figure 22 A 10-year-old male patient with Marfan syndrome. There is mediastinal enlargement and rotoscoliosis in the thoracolumbar region on posteroanterior chest radiograph.

DOI: 10.12998/wjcc.v11.i12.2637

Figure 23 Aneurysmatic dilatation. A: Aneurysmatic dilatation is observed in the aortic root in the axial; B: Coronal images in the computed tomography Angiography.

LYMPHADENOPATHY

Right paratracheal, peribronchial, aortopulmonary window, hilar, and subcarinal lymph nodes are

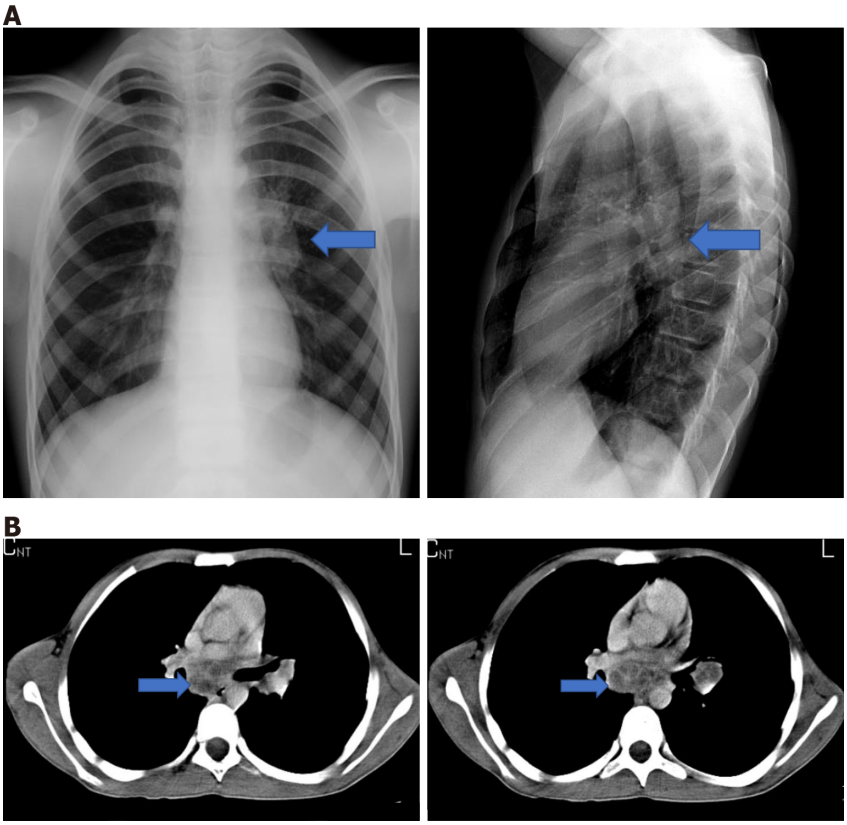

DOI: 10.12998/wjcc.v11.i12.2637

Figure 24 A 16-year-old male patient with tuberculosis. A: There is fever and weight loss. Left hilar LAP is seen on bidirectional chest radiograph (blue arrow). B: Subcarinal and left hilar necrotic lymphadenopathies (blue arrow) are observed in the axial plane computed tomography examination of the same patient.

DOI: 10.12998/wjcc.v11.i12.2637

Figure 25 An 8-year-old female patient followed up with neuroblastoma. Mediastinal enlargement and tracheal deviation are observed in posteroanterior chest radiograph.

situated in the visceral area. The most important causes of lymphadenopathy in children are infections and malignancies. While direct radiography can show symptoms of increased density, mediastinal expansion, compression, or deviation depending on its size, it is also apparent in soft tissue density as an expanded solitary or conglomerating homogenous or heterogeneous solid mass. Lymph node involvement in cancers can be a primary or distant metastasis[21]. Wilms tumor, Ewing sarcoma and osteosarcoma are the most common causes of metastatic lymphadenopathy in children[14]. Lymph nodes may be cystic or calcific. Cystic content indicates necrosis and is often seen in tuberculosis, fungal infections and malignancies such as seminoma, rhabdomyosarcoma[47] (Figures 24-26). Calcified lymph nodes can be seen in granulomatous infections or osteosarcoma, mucinous ovarian carcinoma, and papillary carcinoma of the thyroid[48]. In Hodgkin lymphoma, lymph node calcification may develop after treatment[21].

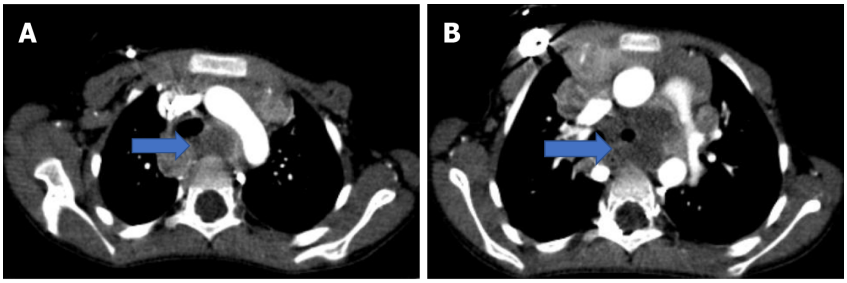

DOI: 10.12998/wjcc.v11.i12.2637

Figure 26 The axial computed tomography images. A and B: In the axial computed tomography images, necrotic lymphadenopathies (blue arrow) are present in paratracheal, precarinal and subcarinal areas; B: They deviate the trachea anteriorly and invade the left bronchus.

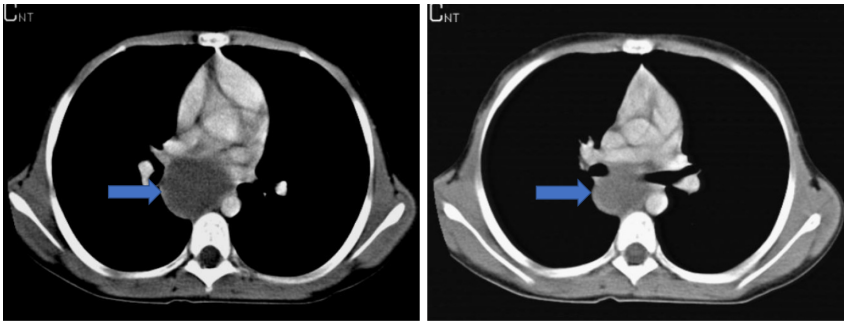

DOI: 10.12998/wjcc.v11.i12.2637

Figure 27 A 15-year-old female patient with bronchogenic cyst (blue arrow). A 15-year-old female has a complaint of intermittent cough. Axial computed tomography images of the patient at different levels show a cyst located posterior to the right hilum (blue arrow).

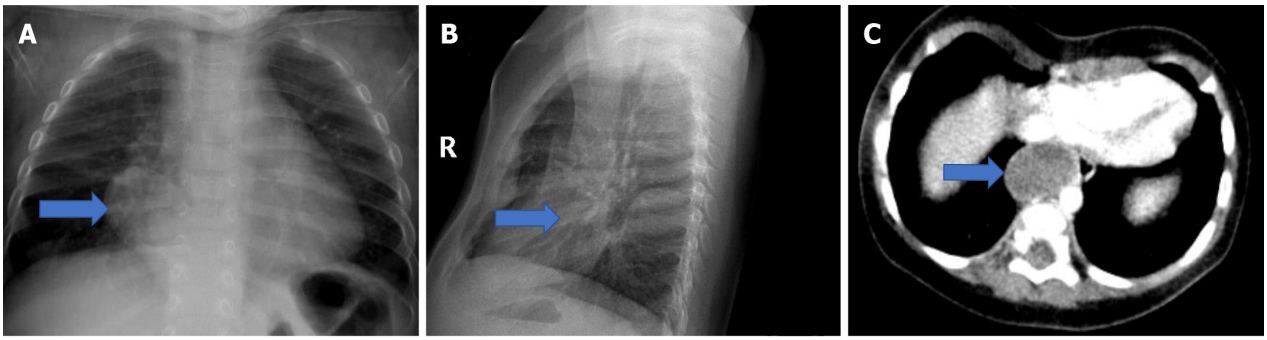

DOI: 10.12998/wjcc.v11.i12.2637

Figure 28 A 6 mo old male patient. A: On posteroanterior chest radiograph right paravertebral; B: Lateral radiograph posteriorly located smooth-contoured density (blue arrow) is observed; C: Esophageal duplication cyst (blue arrow). In the axial computed tomography images of the same patient, a lobulated contoured cyst is observed in the middle mediastinum, adjacent to the esophagus, and it extends into the posterior mediastinum.

FOREGUT DUPLICATION CYST

Foregut duplication cysts are developmental malformations that occur during embryogenesis of the tracheobronchial tree, esophagus, and vertebral column. Esophageal duplication cyst and neuroenteric cyst are two subtypes of bronchiogenic cyst.

Bronchogenic cyst is the most common cyst of the mediastinum. It is seen in approximately 42% of children and the most common location is the middle mediastinum[49]. It frequently appears in the paratracheal, subcarinal, and hilus of the middle mediastinum, with intrapulmonary localisation occurring less frequently (Figures 27 and 28A).

The incidence of esophageal duplication cyst (Figures 28 and 29) is reported as one in 8200 Live births [50]. It is most commonly seen in the lower 1/3 of the esophagus, and the cysts do not show any relation with the esophageal lumen at a rate of 90%[51]. It is localized in the esophageal wall or in its immediate vicinity.

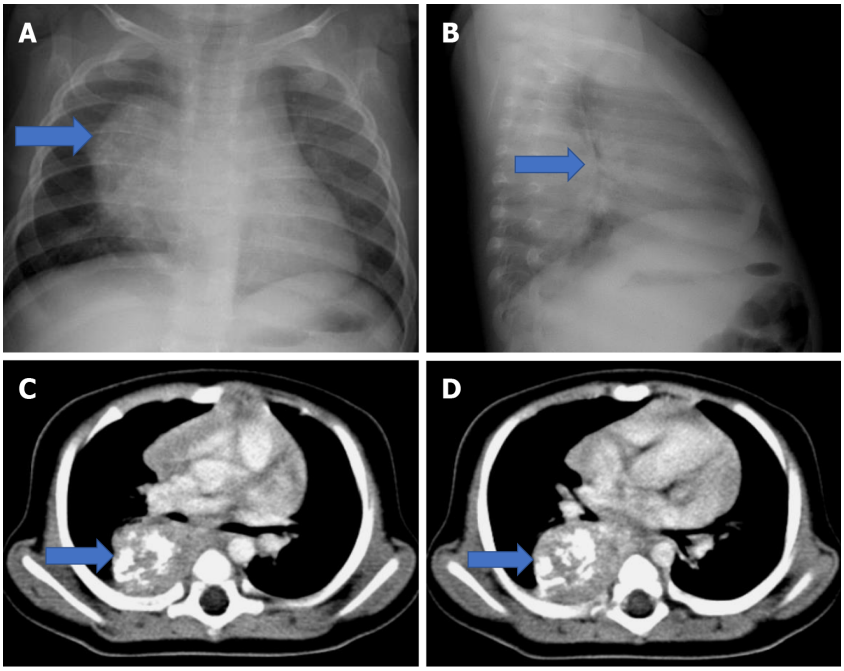

DOI: 10.12998/wjcc.v11.i12.2637

Figure 29 A 7 mo old girl with Neuroblastoma. He is admitted to the hospital because of cough and wheezing. A: On posteroanterior chest radiograph (blue arrow) the mass is seen on the right paravertebral area; B: On the lateral radiograph a posteriorly located mass with a smooth outer contour and calcifications (blue arrow) is seen; C and D: In the axial computed tomography images of the same patient, a homogeneous mass with smooth contours and punctate-coarse calcifications (blue arrow) is observed in the paravertebral distance. The mass extends to the midline and mild compression is detected on the right main bronchus.

Neuroenteric cyst is the rarest type. It is located in the posterior mediastinum 90% and mostly localized at the superior carina level. It may be associated with vertebral anomalies such as hemivertebrae, butterfly vertebra, and scoliosis[4,52].

Foregut duplication cysts are asymptomatic when they are small in size. However, by compressing nearby structures, big lesions may exhibit symptoms as chest discomfort, dysphagia, and dyspnea[53]. Although they are seen as a smooth-contoured density on the direct graphy, they may cause compression-related findings depending on the size of the lesion. On the other hand, CT is observed as a single lesion with oval or round, smooth contours, thin walls, and fluid density. Typically, wall contrast does not appear. Hemorrhage or the presence of protein cause the fluid density to increase[21,53].

PARAVERTEBRAL DISTANCE (POSTERIOR MEDIASTINAL) LESIONS

Approximately 30%-40% of mediastinal masses are located in the posterior mediastinum[36] and 85%-90% of the lesions are of neurogenic origin[52,54]. Neurogenic tumors consist of sympathetic ganglion tumors, peripheral nerve sheath tumors and paragangliomas. However, neuroblastoma, ganglioneuroblastoma and ganglioneuroma constitute the majority of these tumors from sympathetic ganglion tumors. Neuroblastoma and ganglioneuroblastoma are malignant, while ganglioneuroma is benign. Imaging findings are similar in these tumors, but demographic features may be helpful in the differential diagnosis[16]. Age of onset for neuroblastoma is three years, for ganglioneuroblastoma it is before ten years, and for ganglineuroma it is beyond ten years[22]. Neurogenic tumors are observed as paravertebral vertical elongated density on direct radiography. Its outer contour is smooth and convex. In addition, erosion in the vertebral body, rib, enlargement-erosion in the neural foramen and an increase in the intercostal distance may also be detected[22,35]. Calcification is observed at a rate of 30%[21,36]. On CT, calcification is seen in 80%-90% of neuroblastoma and 42%-60% in ganglioneuroma[55,56]. On CT, these tumors can be seen as a well-contoured mass containing calcifications in the paravertebral area (Figures 29 and 30). They can be homogeneous or heterogeneous due to necrosis and hemorrhage. Depending on the size of the mass, compression findings, rib erosion, neural foramen invasion and extension into the spinal canal are also displayed on CT (Figure 31). However, MRI is superior to CT in showing the extension into the spinal canal[14] (Figure 32).

As a result, a wide variety of pathologies occur due to different tissues and organs located in the mediastinum. Imaging methods play an important role in the classification and evaluation of these pathologies. It should be remembered that it will result in congenital vascular diseases in children as well as mass-like imaging abnormalities in normal organs like the thymus.

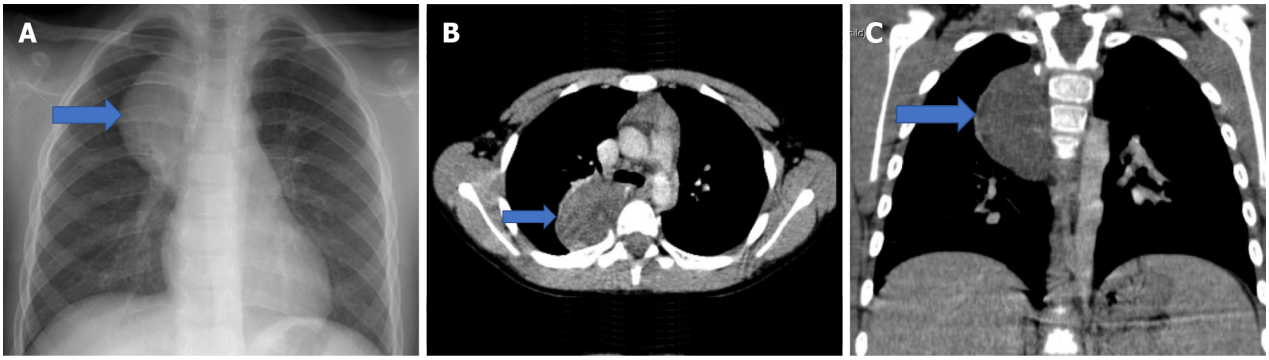

DOI: 10.12998/wjcc.v11.i12.2637

Figure 30 A 6-year-old female patient with Ganglioneuroma. There is a cough complaint that has been going on for 3 mo. Posteroanterior chest radiograph shows a density (blue arrow) of paravertebral, well-contoured mass causing enlargement of the mediastinum on the right; B and C: In the axial and coronal computed tomography images of the same patient, a well-contoured, homogeneous mass (blue arrow) is observed in the paravetebral distance on the right.

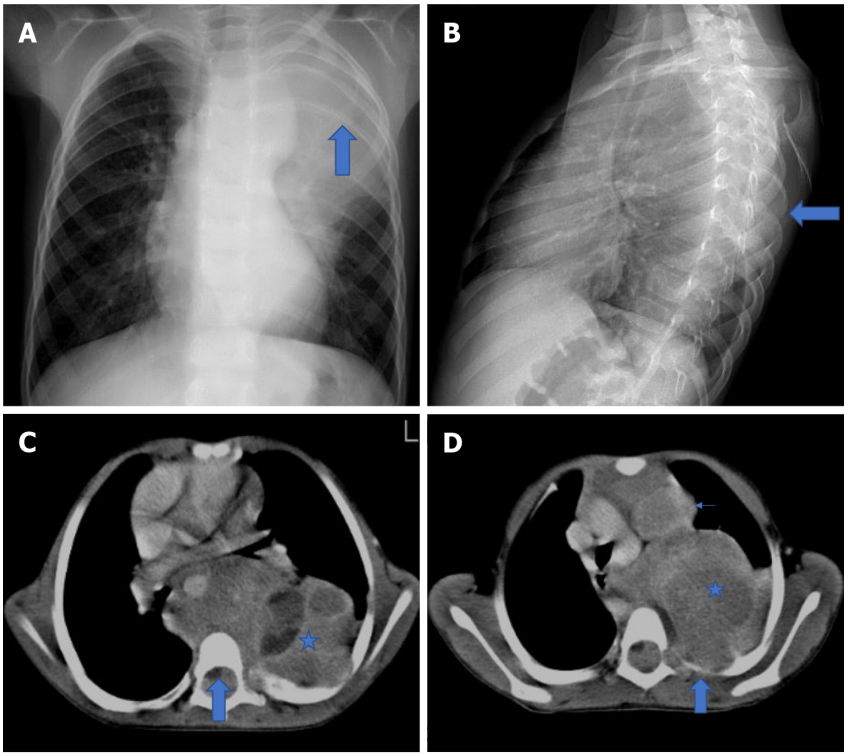

DOI: 10.12998/wjcc.v11.i12.2637

Figure 31 A 5-year-old girl with Ganglioneuroblastoma. There are complaints of cough and left flank pain. A: A lobulated contoured mass lesion is observed in the Posteroanterior chest radiograph (blue arrow) that causes mediastinal enlargement on the left, deviates the trachea to the right; B: It is seen posteriorly on the lateral radiograph and causes erosion in the ribs (blue arrow); C and D: In the axial computed tomography images of the same patient, a heterogeneous mass lesion is seen (blue star).

CONCLUSION

The aim of the study is to ensure that physicians who are at the diagnostic level are more careful in terms of differential diagnoses and to support them with imaging methods.

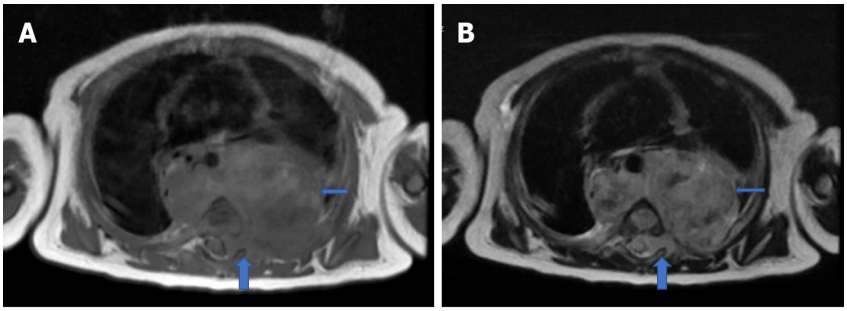

DOI: 10.12998/wjcc.v11.i12.2637

Figure 32 A 4-mo-old male patient diagnosed with neuroblastoma. A: A heterogeneous mass is observed on both sides in the paravertebral area in T1W-weighted; B: T2W-weighted sections in the axial plane. The descending aorta is surrounded by the mass (thin blue arrow) and pushed anteriorly. It is also noteworthy that the mass invades the left neural foramen, extending into the spinal canal and compressing the spinal cord (A and B, thick blue arrow).

FOOTNOTES

Author contributions: Gulmez AO and Aydin S contributed equally to this work; Çinar HG, Üner C, Aydin S designed the research study; Gulmez AO carried out the research; Aydin S contributed new reagents and analytical tools; Çinar HG, Üner C analyzed the data and wrote the draft; All authors have read and approved the final draft.

Conflict-of-interest statement: All the authors report no relevant conflicts of interest for this article.

Country/Territory of origin: Turkey

ORCID number: Hasibe Gökçe Çinar 0000-0003-2687-1544; Ali Osman Gulmez 0000-0001-7050-1765; Çiğdem Üner 0000-0002-4846-7764; Sonay Aydin 0000-0002-3812-6333.

S-Editor: Li L
L-Editor: A
P-Editor: Chen YX

REFERENCES

1 **Lerman J**. Anterior mediastinal masses in children. *Seminars in Anesthesia, Perioperative Medicine and Pain* 2007; **26**: 133-140 [DOI: 10.1053/j.sane.2007.06.003]
2 **Verma S**, Kalra K, Rastogi S, Sidhu HS. Clinical approach to childhood mediastinal tumors and management. *Mediastinum* 2020; **4**: 21 [PMID: 35118289 DOI: 10.21037/med-19-82]
3 **Güler S**, Demirkaya M, Sevinir B. Çocukluk çağı mediastinal kitlelere yaklaşım. J Curr Pediatr 2016;14:30-36 [DOI: 10.4274/jcp.81905]
4 **Laurent F**, Latrabe V, Lecesne R, Zennaro H, Airaud JY, Rauturier JF, Drouillard J. Mediastinal masses: diagnostic approach. *Eur Radiol* 1998; **8**: 1148-1159 [PMID: 9724429 DOI: 10.1007/s003300050525]
5 **Yardımcı AH**, Kılıçkesmez Ö. Mediasten hastalıklarında radyolojik değerlendirme. Güncel Göğüs Hastalıkları Serisi 2020; 8: 11-30
6 **Adegboye VO**, Brimmo AI, Adebo OA, Ogunseyinde OO, Obajimi MO. The place of clinical features and standard chest radiography in evaluation of mediastinal masses. *West Afr J Med* 2003; **22**: 156-160 [PMID: 14529228 DOI: 10.4314/wajm.v22i2.27939]
7 **Ahn JM**, Lee KS, Goo JM, Song KS, Kim SJ, Im JG. Predicting the histology of anterior mediastinal masses: comparison of chest radiography and CT. *J Thorac Imaging* 1996; **11**: 265-271 [PMID: 8892196 DOI: 10.1097/00005382-199623000-00004]
8 **Lee EY**. Evaluation of non-vascular mediastinal masses in infants and children: an evidence-based practical approach. *Pediatr Radiol* 2009; **39** Suppl 2: S184-S190 [PMID: 19308383 DOI: 10.1007/s00247-008-1108-2]
9 **Brillantino C**, Rossi E, Tambaro FP, Minelli R, Bignardi E, Cremone G, Zeccolini R, Zeccolini M. Clinical and Imaging Findings Useful in the Differential Diagnosis of Most Common Childhood Mediastinal Tumors. *Trans Med* 2019; **9**: 207
10 **Carter BW**, Benveniste MF, Madan R, Godoy MC, de Groot PM, Truong MT, Rosado-de-Christenson ML, Marom EM. ITMIG Classification of Mediastinal Compartments and Multidisciplinary Approach to Mediastinal Masses. *Radiographics* 2017; **37**: 413-436 [PMID: 28129068 DOI: 10.1148/rg.2017160095]

11 **Nursun Özcan**. Çocuklarda toraks radyolojisi. In: Aslan AT, Kiper N (eds). Çocuk Göğüs Hastalıklarında Tanı Yöntemleri. 2016 TUSAD. *Türkiye Solunum Araştırmaları Derneği* 2016; 26-36

12 **Kapur S**, Bhalla AS, Jana M. Pediatric Chest MRI: A Review. *Indian J Pediatr* 2019; **86**: 842-853 [PMID: 30719641 DOI: 10.1007/s12098-018-02852-w]

13 **Gun F**, Erginel B, Unüvar A, Kebudi R, Salman T, Celik A. Mediastinal masses in children: experience with 120 cases. *Pediatr Hematol Oncol* 2012; **29**: 141-147 [PMID: 22376017 DOI: 10.3109/08880018.2011.646385]

14 **Thacker PG**, Mahani MG, Heider A, Lee EY. Imaging Evaluation of Mediastinal Masses in Children and Adults: Practical Diagnostic Approach Based on A New Classification System. *J Thorac Imaging* 2015; **30**: 247-267 [PMID: 26086589 DOI: 10.1097/RTI.0000000000000161]

15 **Wright CD**. Mediastinal tumors and cysts in the pediatric population. *Thorac Surg Clin* 2009; **19**: 47-61, vi [PMID: 19288820 DOI: 10.1016/j.thorsurg.2008.09.014]

16 **Davies-Tuck ML**, Wluka AE, Teichtahl AJ, Martel-Pelletier J, Pelletier JP, Jones G, Ding C, Davis SR, Cicuttini FM. Association between meniscal tears and the peak external knee adduction moment and foot rotation during level walking in postmenopausal women without knee osteoarthritis: a cross-sectional study. *Arthritis Res Ther* 2008; **10**: R58 [PMID: 18492234 DOI: 10.1186/ar2428]

17 **Aslan A**, Yıkılmaz A. Normal ve patolojik pediatrik akciğer ve toraks radyografisi. Türk Radyoloji Seminerleri. *Trd Sem* 2017; **5**: 98-128 [DOI: 10.5152/trs.2017.460]

18 **Nasseri F**, Eftekhari F. Clinical and radiologic review of the normal and abnormal thymus: pearls and pitfalls. *Radiographics* 2010; **30**: 413-428 [PMID: 20228326 DOI: 10.1148/rg.302095131]

19 **Manchanda S**, Bhalla AS, Jana M, Gupta AK. Imaging of the pediatric thymus: Clinicoradiologic approach. *World J Clin Pediatr* 2017; **6**: 10-23 [PMID: 28224091 DOI: 10.5409/wjcp.v6.i1.10]

20 **Çolak E**, Özkan B. Multidetector Computed Tomographic Evaluation of the Normal Characteristics of the Thymus in the Pediatric Population. *J Belg Soc Radiol* 2022; **106**: 110 [PMID: 36447629 DOI: 10.5334/jbsr.2971]

21 **Ranganath SH**, Lee EY, Restrepo R, Eisenberg RL. Mediastinal masses in children. *AJR Am J Roentgenol* 2012; **198**: W197-W216 [PMID: 22358017 DOI: 10.2214/AJR.11.7027]

22 **Biko DM**, Lichtenberger JP 3rd, Rapp JB, Khwaja A, Huppmann AR, Chung EM. Mediastinal Masses in Children: Radiologic-Pathologic Correlation. *Radiographics* 2021; **41**: E164 [PMID: 34469225 DOI: 10.1148/rg.2021219008]

23 **Priola AM**, Priola SM, Ciccone G, Evangelista A, Cataldi A, Gned D, Pazè F, Ducco L, Moretti F, Brundu M, Veltri A. Differentiation of rebound and lymphoid thymic hyperplasia from anterior mediastinal tumors with dual-echo chemical-shift MR imaging in adulthood: reliability of the chemical-shift ratio and signal intensity index. *Radiology* 2015; **274**: 238-249 [PMID: 25105246 DOI: 10.1148/radiol.14132665]

24 **el-Sharkawi AM**, Patel B. Management of residual thymic cysts in patients treated for mediastinal Hodgkin's disease. *Thorax* 1995; **50**: 1118-1119 [PMID: 7491566 DOI: 10.1136/thx.50.10.1118]

25 **Strollo DC**, Rosado-de-Christenson ML. Tumors of the thymus. *J Thorac Imaging* 1999; **14**: 152-171 [PMID: 10404501 DOI: 10.1097/00005382-199907000-00002]

26 **Hara M**, Suzuki H, Ohba S, Satake M, Ogino H, Itoh M, Yamakawa Y, Tateyama H. A Case of Thymic Cyst Associated with Thymoma and Intracystic Dissemination. *Radiation Medicine* 2000; **18**: 311-313. (25)

27 **King RM**, Telander RL, Smithson WA, Banks PM, Han MT. Primary mediastinal tumors in children. *J Pediatr Surg* 1982; **17**: 512-520 [PMID: 7175638 DOI: 10.1016/S0022-3468(82)80100-0]

28 **Fonseca AL**, Ozgediz DE, Christison-Lagay ER, Detterbeck FC, Caty MG. Pediatric thymomas: report of two cases and comprehensive review of the literature. *Pediatr Surg Int* 2014; **30**: 275-286 [PMID: 24322668 DOI: 10.1007/s00383-013-3438-x]

29 **Siegel DA**, King J, Tai E, Buchanan N, Ajani UA, Li J. Cancer incidence rates and trends among children and adolescents in the United States, 2001-2009. *Pediatrics* 2014; **134**: e945-e955 [PMID: 25201796 DOI: 10.1542/peds.2013-3926]

30 **Ward E**, DeSantis C, Robbins A, Kohler B, Jemal A. Childhood and adolescent cancer statistics, 2014. *CA Cancer J Clin* 2014; **64**: 83-103 [PMID: 24488779 DOI: 10.3322/caac.21219]

31 **Pui CH**, Behm FG, Singh B, Schell MJ, Williams DL, Rivera GK, Kalwinsky DK, Sandlund JT, Crist WM, Raimondi SC. Heterogeneity of presenting features and their relation to treatment outcome in 120 children with T-cell acute lymphoblastic leukemia. *Blood* 1990; **75**: 174-179 [PMID: 2136802 DOI: 10.1182/blood.V75.1.174.bloodjournal751174]

32 **Smith WT**, Shiao KT, Varotto E, Zhou Y, Iijima M, Anghelescu DL, Cheng C, Jeha S, Pui CH, Kaste SC, Inaba H. Evaluation of Chest Radiographs of Children with Newly Diagnosed Acute Lymphoblastic Leukemia. *J Pediatr* 2020; **223**: 120-127.e3 [PMID: 32711740 DOI: 10.1016/j.jpeds.2020.04.003]

33 **Lakatos K**, Herbrüggen H, Pötschger U, Prosch H, Minkov M. Radiological features of thymic langerhans cell histiocytosis. *Pediatr Blood Cancer* 2013; **60**: E143-E145 [PMID: 23813898 DOI: 10.1002/pbc.24640]

34 **Singh AK**, Sargar K, Restrepo CS. Pediatric Mediastinal Tumors and Tumor-Like Lesions. *Semin Ultrasound CT MR* 2016; **37**: 223-237 [PMID: 27261347 DOI: 10.1053/j.sult.2015.11.005]

35 **McCarville MB**. Malignant pulmonary and mediastinal tumors in children: differential diagnoses. *Cancer Imaging* 2010; **10** Spec no A: S35-S41 [PMID: 20880793 DOI: 10.1102/1470-7330.2010.9015]

36 **Franco A**, Mody NS, Meza MP. Imaging evaluation of pediatric mediastinal masses. *Radiol Clin North Am* 2005; **43**: 325-353 [PMID: 15737372 DOI: 10.1016/j.rcl.2005.01.002]

37 **Billmire DF**. Germ cell, mesenchymal, and thymic tumors of the mediastinum. *Semin Pediatr Surg* 1999; **8**: 85-91 [PMID: 10344305 DOI: 10.1016/S1055-8586(99)70022-3]

38 **Barksdale EM Jr**, Obokhare I. Teratomas in infants and children. *Curr Opin Pediatr* 2009; **21**: 344-349 [PMID: 19417664 DOI: 10.1097/MOP.0b013e32832b41ee]

39 **Yalçın B**, Demir HA, Tanyel FC, Akçören Z, Varan A, Akyüz C, Kutluk T, Büyükpamukçu M. Mediastinal germ cell tumors in childhood. *Pediatr Hematol Oncol* 2012; **29**: 633-642 [PMID: 22877235 DOI: 10.3109/08880018.2012.713084]

40 **Ueno T**, Tanaka YO, Nagata M, Tsunoda H, Anno I, Ishikawa S, Kawai K, Itai Y. Spectrum of germ cell tumors: from head to toe. *Radiographics* 2004; **24**: 387-404 [PMID: 15026588 DOI: 10.1148/rg.242035082]

41 **Levitt RG**, Husband JE, Glazer HS. CT of primary germ-cell tumors of the mediastinum. *AJR Am J Roentgenol* 1984; **142**: 73-78 [PMID: 6318540 DOI: 10.2214/ajr.142.1.73]

42 **Logothetis CJ**, Samuels ML, Selig DE, Dexeus FH, Johnson DE, Swanson DA, von Eschenbach AC. Chemotherapy of extragonadal germ cell tumors. *J Clin Oncol* 1985; **3**: 316-325 [PMID: 2579212 DOI: 10.1200/JCO.1985.3.3.316]

43 **Nichols CR**, Heerema NA, Palmer C, Loehrer PJ Sr, Williams SD, Einhorn LH. Klinefelter's syndrome associated with mediastinal germ cell neoplasms. *J Clin Oncol* 1987; **5**: 1290-1294 [PMID: 3040921 DOI: 10.1200/JCO.1987.5.8.1290]

44 **Tecce PM**, Fishman EK, Kuhlman JE. CT evaluation of the anterior mediastinum: spectrum of disease. *Radiographics* 1994; **14**: 973-990 [PMID: 7991827 DOI: 10.1148/radiographics.14.5.7991827]

45 **Karakurt**, C. Aortic Aneurysm in Children and Adolescents. In: Amalinei, C., editor. Aortic Aneurysm - Recent Advances [Internet]. London: IntechOpen; 2013 [DOI: 10.5772/53383]

46 **Carter RAA**, West N, Heitz A, Joll CA. An analytical method for the analysis of trihalomethanes in ambient air using solid-phase microextraction gas chromatography-mass spectrometry: An application to indoor swimming pool complexes. *Indoor Air* 2019; **29**: 499-509 [PMID: 30844099 DOI: 10.1111/ina.12551]

47 **Siegel Marilyn J**. Pediatric Body Ct. 2nd ed. Wolters Kluwer Health - Lippincott Williams & Wilkins 2007

48 **Glazer HS**, Molina PL, Siegel MJ, Sagel SS. High-attenuation mediastinal masses on unenhanced CT. *AJR Am J Roentgenol* 1991; **156**: 45-50 [PMID: 1898569 DOI: 10.2214/ajr.156.1.1898569]

49 **McAdams HP**, Kirejczyk WM, Rosado-de-Christenson ML, Matsumoto S. Bronchogenic cyst: imaging features with clinical and histopathologic correlation. *Radiology* 2000; **217**: 441-446 [PMID: 11058643 DOI: 10.1148/radiology.217.2.r00nv19441]

50 **Cuch B**, Nachulewicz P, Wieczorek AP, Wozniak M, Pac-Kozuchowska E. Esophageal Duplication Cyst Treated Thoracoscopically During the Neonatal Period: Clinical Case Report. *Medicine (Baltimore)* 2015; **94**: e2270 [PMID: 26656375 DOI: 10.1097/MD.0000000000002270]

51 **Wootton-Gorges SL**, Eckel GM, Poulos ND, Kappler S, Milstein JM. Duplication of the cervical esophagus: a case report and review of the literature. *Pediatr Radiol* 2002; **32**: 533-535 [PMID: 12107589 DOI: 10.1007/s00247-002-0693-8]

52 **Strollo DC**, Rosado-de-Christenson ML, Jett JR. Primary mediastinal tumors: part II. Tumors of the middle and posterior mediastinum. *Chest* 1997; **112**: 1344-1357 [PMID: 9367479 DOI: 10.1378/chest.112.5.1344]

53 **Jeung MY**, Gasser B, Gangi A, Bogorin A, Charneau D, Wihlm JM, Dietemann JL, Roy C. Imaging of cystic masses of the mediastinum. *Radiographics* 2002; **22** Suppl: S79-S93 [PMID: 12376602 DOI: 10.1148/radiographics.22.suppl_1.g02oc09s79]

54 **Meza MP**, Benson M, Slovis TL. Imaging of mediastinal masses in children. *Radiol Clin North Am* 1993; **31**: 583-604 [PMID: 8497592 DOI: 10.1016/S0033-8389(22)02607-0]

55 **Lonergan GJ**, Schwab CM, Suarez ES, Carlson CL. Neuroblastoma, ganglioneuroblastoma, and ganglioneuroma: radiologic-pathologic correlation. *Radiographics* 2002; **22**: 911-934 [PMID: 12110723 DOI: 10.1148/radiographics.22.4.g02jl15911]

56 **Scherer A**, Niehues T, Engelbrecht V, Mödder U. Imaging diagnosis of retroperitoneal ganglioneuroma in childhood. *Pediatr Radiol* 2001; **31**: 106-110 [PMID: 11214677 DOI: 10.1007/s002470000381]

Published by **Baishideng Publishing Group Inc**
7041 Koll Center Parkway, Suite 160, Pleasanton, CA 94566, USA
Telephone: +1-925-3991568
E-mail: bpgoffice@wjgnet.com
Help Desk: https://www.f6publishing.com/helpdesk
https://www.wjgnet.com